

Multiple reflection interference experiments violating the conservation of energy law

Kazufumi Sakai
ksakai1958@gmail.com

The conservation law of energy asserts that the total energy must always remain constant, even when its form changes. This conservation law also holds in electromagnetism (optics), where the total energy of light incident on and output from a system must be equal. However, we have found a phenomenon in which the total energy of the interference light emitted from a multiple-reflection interferometer is greater than the energy of the incident light. This increase is stable in time and can be explained by wave optics. The energy conservation law is valid when averaged over a region sufficiently wider than the interference fringe period, but when the beam width is narrower than the fringe period, the total light intensity increases or decreases and the conservation law does not hold.

PACS numbers:

I. INTRODUCTION

It is well known that when light is incident on a thin film, the sum of the energy of the reflected and transmitted waves produced by multiple reflections equals the total energy of the incident light[1]. This is an example of electromagnetism (or wave optics) conforming to the law of conservation of energy. This conservation law has been confirmed to hold in most areas of physics, with the exception of systems that do not have time translation symmetry, etc.[2–5]

When the relative angle between a half-mirror and a mirror is sufficiently small in a multiple-reflection system using a half-mirror and a mirror, the distance between bright lines of interference fringes extends from a few millimeters to more than ten millimeters. We found that when a laser beam with a width narrower than the distance between the bright lines is incident on this device, the total light intensity increases or decreases depending on the position of the incident laser beam. Although this phenomenon seems impossible to explain by electromagnetism because it violates the conservation of energy law, this paper shows that this phenomenon can be explained by using wave optics. In Chapter 2, we describe the experimental setup and measurement results to verify this effect. We observed an increase in light intensity by a factor of approximately 1.3.

II. ENERGY INCREASE/DECREASE EFFECT BY MULTIPLE REFLECTION INTERFERENCE

The reflection and transmission of light by the half-mirror and the mirror of the multiple reflection interferometer are shown in Figure 1. A beam vertically incident on the half-mirror is divided into p_0 light reflected by the half-mirror, p_1 light reflected once by the mirror and emitted, p_2 light reflected twice by the mirror, p_3 light reflected three times, and so on. If the relative angle between the half-mirror and the mirror is θ , the light is reflected at angles of 0° , $2\theta^\circ$, $4\theta^\circ$, and $6\theta^\circ$, respectively.

If the distance between the half-mirror and the mirror at $x = 0$ is d and the incident position of the beam is x , then α_0 in Figure 1 is given by

$$\alpha_0 = (d - x \tan \theta) \quad (1)$$

Using this α_0 , the optical path lengths ($h_1 = A_0 \sim A_1, h_2 = A_1 \sim A_2, \dots$) that light travels between the half-mirror and the mirror are given by the following equations, respectively.

$$\begin{aligned} h_1 &= \alpha_0 \cos \theta \left(\frac{1}{\cos(0\theta) \cos(\theta)} + \frac{1}{\cos(\theta) \cos(2\theta)} \right) \\ h_2 &= \alpha_0 \cos \theta \left(\frac{1}{\cos(2\theta) \cos(3\theta)} + \frac{1}{\cos(3\theta) \cos(4\theta)} \right) \\ h_3 &= \alpha_0 \cos \theta \left(\frac{1}{\cos(4\theta) \cos(5\theta)} + \frac{1}{\cos(5\theta) \cos(6\theta)} \right) \\ &\vdots \\ h_n &= \frac{\alpha_0 \cos \theta}{\cos((2n-1)\theta)} \left(\frac{1}{\cos((2n-2)\theta)} + \frac{1}{\cos(2n\theta)} \right) \end{aligned} \quad (2)$$

Therefore, the total optical path length s_m of reflected light p_m to the observation surface is given by

$$\begin{aligned} s_m &= \sum_{n=1}^m \frac{\alpha_0 \cos \theta}{\cos((2n-1)\theta)} \left(\frac{1}{\cos((2n-2)\theta)} + \frac{1}{\cos(2n\theta)} \right) \\ &+ \frac{L}{\cos(2m\theta)} \end{aligned} \quad (3)$$

Here, the distance from the surface of the half-mirror to the observation surface is L . However, these reflected beams do not intersect (i.e., do not interfere) because the angles of each reflected beam are different, as can be seen from Figure 1. In order for the reflected waves to intersect at coordinate x , the incident position (in the x -axis direction) of each reflected wave must be corrected. Let x_m be the corrected incident light position of each

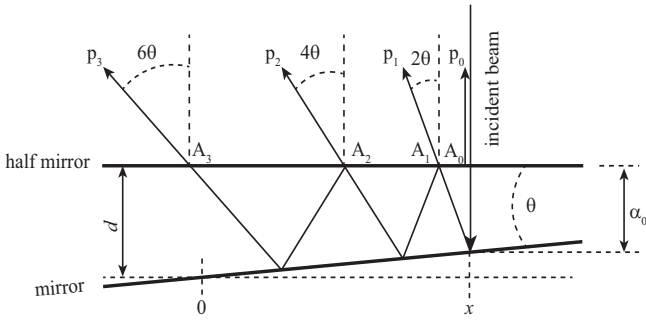


FIG. 1: Schematic diagram of multiple reflections by a half-mirror and a mirror: light incident at point A_0 is repeatedly reflected between the mirror and the half-mirror and then emitted in each direction. The distance between the mirror and the half-mirror at $x = 0$ is d and the angle between the mirror and the half-mirror is θ .

reflected light, and let α_m be the corresponding α_0 . Then α_m must satisfy the following equation.

$$\begin{aligned} \alpha_m &= d - x_m \tan \theta \\ x &= x_m \\ &- \sum_{n=1}^m \frac{\alpha_m \cos \theta}{\cos((2n-1)\theta)} (\tan((2n-2)\theta) + \tan(2n\theta)) \\ &- L \tan(2m\theta) \end{aligned} \quad (4)$$

The first term is the incident position of the beam, the second term is the distance from the incident position x_m to the output position A_m of the m -th reflected light, and the third term is the horizontal distance from the A_m point to the observation point. Using these terms, the electric field at position x of the observation surface is given by

$$E = -r \exp\left(\frac{-i2\pi L}{\lambda}\right) + r \sum_{m=1}^{\infty} (-r)^m \exp\left(\frac{-i2\pi s_m}{\lambda}\right) \quad (5)$$

where the first term is the light wave reflected at point A_0 . The time component was neglected because of the simultaneous measurement. It was also assumed that the phase changes when light reflects off the upper surface of the half-mirror and that there is no phase change when light reflects off the lower surface (the calculated light intensity would be the same if the situation were reversed). For further simplification, the amplitude reflectance r and amplitude transmittance t were assumed to be equal and $r^2 = t^2 = 1/2$.

Figure 2(a) shows an example of calculated intensity distribution on the observation plane when $L = 185\text{mm}$, $d = 2\text{mm}$, $\theta = 0.0022^\circ$, wavelength = 635nm and $m = 10$. Bright lines of interference appear at intervals of about 8 mm. When the average intensity of the incident beam is 1, the average between bright lines in Figure 2(a) is 1.01, which is almost the same as the average intensity of the incident beam. In other words, when the intensity average is calculated in a region containing

many bright lines, it can be said that the energy of the incident light and the outgoing light is conserved. If the width of the incident beam is narrowed to 2 mm as shown in the dotted line in Figure 2 and the same calculation is performed at two locations, the intensity distributions shown in Figures 2(b-1) and 2(b-2) are obtained, respectively. Although the left and right sides of the graphs are deformed due to beam shift caused by multiple reflections, it can be seen that the waveforms are almost identical to those at the corresponding locations in Figure 2(a). However, it can be seen that the average value of the intensity differs significantly from the intensity average of the incident light.

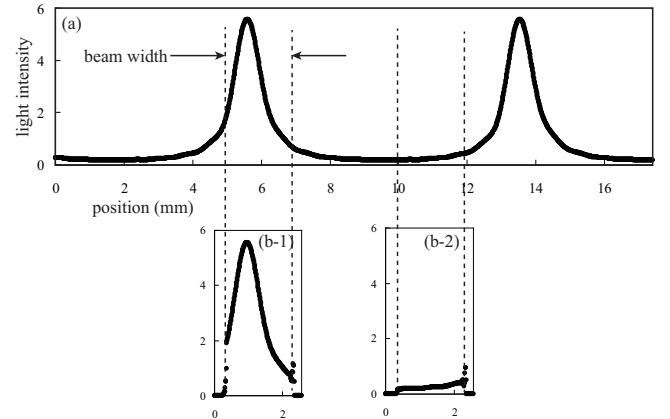


FIG. 2: Example of interference fringes calculated using equation (5): (a) is an example calculation for $L = 185\text{mm}$, $d = 2\text{mm}$, $\theta = 0.0022^\circ$, wavelength = 635nm and $m = 10$. (b-1) and (b) are examples of light intensity calculations when the incident beam width is narrowed to the dotted line width (2 mm). Even when the beam is narrowed, the waveform is almost identical to the waveform at the corresponding position in (a).

Figure 3 is obtained by averaging the intensity of the emitted light when the position of the 2 mm wide beam was moved from left to right at 0.5 mm intervals. The highest value was approximately 3. This means that depending on the incident position of the beam (average intensity = 1), the amount of emitted light is about 3 times greater, and that the law of conservation of energy is violated. This result is an effect that occurs only when the beam width is smaller than the distance between the bright lines of the interference fringes.

Approximating equations (1) to (5) with small θ ($\cos \theta \approx 1, \tan \theta \approx \theta$), we obtain the following equations.

$$\alpha_m \approx \alpha_0 - 2m\theta^2(md + L) \quad (6)$$

$$s_m \approx 2\alpha_0 m + L - (2\theta^2 L)m^2 \quad (7)$$

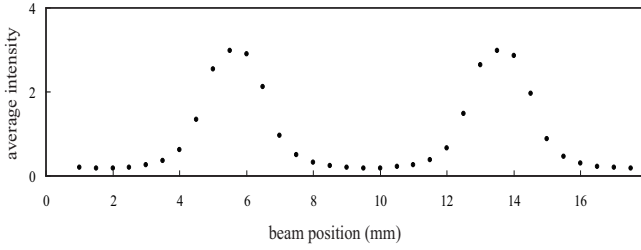


FIG. 3: The average intensity of light when the beam position, indicated by the dotted line in Figure 2, is moved from left to right. When the average intensity of the incident beam is 1, the highest value of the emitted light is about 3. The average value of all points in the figure is $0.99 \approx 1$.

$$\begin{aligned}
 |E|^2 &\approx (r^2 + r^4 + r^6 + \dots) \\
 &+ 2r^3 \cos\left(2\pi \frac{2(d - x\theta) - 2\theta^2 L}{\lambda}\right) + \dots \\
 &= 1 + 2r^3 \cos\left(2\pi \frac{2(d - x\theta) - 2\theta^2 L}{\lambda}\right) + \dots \quad (8)
 \end{aligned}$$

The second term of equation (8) shows that the spacing of interference fringes in the x -axis direction is of the order of $1/\theta$. Similarly, for changes in L and d , the interference fringes change on the order of $1/\theta^2$ and wavelength, respectively. When $\theta = 0$, the phase change is due to the round-trip distance between the half-mirror and the mirror, and the similar equation as for thin-film interference can be obtained. The change with L also indicates that the beam intensity proceeds with an increase or decrease. This property can be used to adjust the intensity at a specific point (region) in space.

III. MULTIPLE REFLECTION INTERFEROMETER AND EXPERIMENTAL RESULTS

Figure 4 shows an interference system using multiple reflections. Light emitted from a laser (635 nm) is spread along a line by a line generator (fan angle = 30°) and passes through a Glan-Thompson polarizer (P polarizer). The P-polarized beam goes straight through the polarizing beam splitter (no reflection), passes through the $\lambda/4$ wave plate, is repeatedly reflected by a half-mirror and mirror, and then passes through the $\lambda/4$ wave plate once again. The beam, which is S-polarized by the wave plate, is perfectly reflected by the polarizing beam splitter, and the total light intensity and the interference image are simultaneously measured by a 10 mm square photo diode (PD) and a charge-coupled device (CCD). A fiberoptic plate (FOP) was used as a screen to observe the interference fringes, with a resolution of $6\mu\text{m}$ and a numerical aperture (NA) of 1.00.

The CCD images of the experimental setup with the slit removed (or when the slit width is about 10 mm) are shown in Figures 5(a) and 5(b). When the mirror

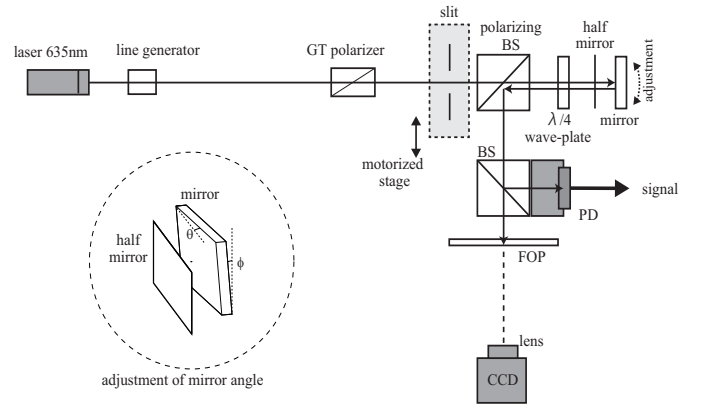


FIG. 4: Multiple-reflection interferometer: laser light passes through a line generator, a polarizer (P polarization), and a slit and travels straight through a polarizing BS. The light reflected by the mirror and half-mirror many times becomes S-polarized by the waveplate and is detected by the CCD and PD.

angle ϕ is 0° , interference fringes are generated, as shown in Figure 5(a), and the interval between them becomes wider when the mirror angle θ is small and gradually narrows as θ is increased. These interference fringes are similar to fringes of equal inclination and Newton rings. When the mirror angle ϕ is not 0° , the interference fringes disappear, and the incident beam is split into multiple beams via multiple reflections to form a linear image, as shown in Figure 5(b).

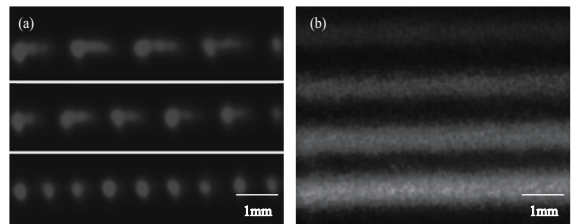


FIG. 5: (a) Interference fringes observed via CCD at $\phi = 0$. Examples of interference fringes at three θ are shown. (b) When $\phi \neq 0$, light reflected by the mirror does not overlap, and multiple independent linear beam images are obtained.

Next, a $500\mu\text{m}$ wide slit is placed. Because the distance from the line generator to the slit is 300mm and the slit width is $500\mu\text{m}$, the spread angle of the light passing through the slit is ± 0.048 degrees. Therefore, the light passing through the slit can be considered nearly parallel. While moving the slit in the direction of the arrow shown in Figure 4 at $50\mu\text{m}$ intervals, the total amount of emitted light was measured with the PD. The results are shown in Figure 6. The black and white circles are the light intensity detected by the PD when $\phi = 0$ and $\phi \neq 0$, respectively. At $\phi \neq 0$, the multiply reflected light reflects independently, so the total light intensity is the incident intensity itself and is almost constant over the entire region. On the other hand, when $\phi = 0$, the

intensity is changing. When the slit is located at A in Figure 6, the intensity decreases from that of the incident beam (about 67 %) and, conversely, increases near point B (about 130 %). This result corresponds to Figure 3. Thus, the same effect as in the calculation using wave optics was confirmed experimentally.

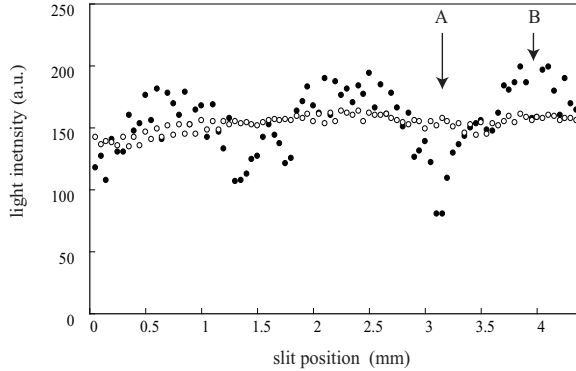


FIG. 6: Light intensity detected by the PD against the position of the beam ($500\mu\text{m}$ width). The distance between the mirror and the half-mirror is about 2 mm, θ is about 0.01 degrees, and the distance between the half-mirror and the FOP is 185 mm. The black circles indicate the light intensity when $\phi \neq 0$ and show fringes, and the white circles indicate the light intensity when $\phi = 0$ and show fringes, and the white circle represents the incident light intensity, which is almost constant regardless of the beam position because the light does not overlap. At beam position A, the emitted light (black circle) decreases from the incident light (white circle), and at B, the emitted light increases.

IV. CONCLUSION

Theoretical and experimental studies have shown that the energy of the emitted beam may be higher than the energy of the incident beam using the multiple reflection interferometer. The primary cause of this effect is the use of beam-widths shorter than the interference fringe period.

However, this result is very strange when considered in terms of photon number. Since this device contains no nonlinear elements, the number of photons must be conserved, but the experimental results show that this number is increasing or decreasing. Where these photons originated is a serious question. The change in the light intensity in the L direction from equation (8) also indicates that the interference light is traveling with an increase or decrease in the number of photons. We suspect that different spaces may be involved in these mysterious phenomena.

On the other hand, the energy-increasing effect is industrially very useful. With the development of low-loss optical elements and improved efficiency of optical-electrical energy conversion, we believe this effect can make a significant contribution to solving energy-related problems.

-
- [1] F. Jenkins and H. White, *Fundamentals of Optics* (McGraw-Hill Science Engineering, 2001).
 - [2] Richard Feynman, *The Feynman Lectures on Physics Vol I* (Addison-Wesley, 1970).
 - [3] Ruth Hagengruber, *Émilie du Chatelet between Leibniz and Newton* (Springer 2011).
 - [4] Robyn Arianrhod, *Seduced by Logic : Émilie du Châtelet,*

- Mary Somerville and the Newtonian revolution (New York: Oxford University Press, 2012)
- [5] Edward Witten, "A new proof of the positive energy theorem", *Communications in Mathematical Physics*. 80 (3), 381, 1981.